

Influence of oxygen vacancy on the electronic structure of HfO_2 film

Deok-Yong Cho,¹ Jae-Min Lee,¹ S.-J. Oh,^{1,*} Hoyoung Jang,² J.-Y. Kim,³ J.-H. Park,^{2,3} and A. Tanaka⁴

¹*CSCMR & School of Physics and Astronomy, Seoul National University, Seoul 151-742, Korea*

²*eSSC & Department of Physics, Pohang University of Science and Technology, Pohang 790-784, Korea*

³*Pohang Accelerator Laboratory & Pohang University of Science and Technology, Pohang 790-784, Korea*

⁴*Department of Quantum Matter, ADISM, Hiroshima University, Higashi-Hiroshima 739-8526, Japan*

We investigated the unoccupied part of the electronic structure of the oxygen-deficient hafnium oxide ($\text{HfO}_{\sim 1.8}$) using soft x-ray absorption spectroscopy at O K and Hf N_3 edges. Band-tail states beneath the unoccupied Hf $5d$ band are observed in the O K -edge spectra; combined with ultraviolet photoemission spectrum, this indicates the non-negligible occupation of Hf $5d$ state. However, Hf N_3 -edge magnetic circular dichroism spectrum reveals the absence of a long-range ferromagnetic spin order in the oxide. Thus the small amount of d electron gained by the vacancy formation does not show inter-site correlation, contrary to a recent report [M. Venkatesan *et al.*, Nature **430**, 630 (2004)].

PACS numbers: 78.70.Dm, 73.20.Hb, 73.61.Ng, 75.70.-i

Oxygen vacancy in a large-bandgap oxide changes the electrical characteristics by forming defect states inside the bandgap. Depending on the position and density of the defect energy levels, the chemical potential of the oxide - frequently identified with the Fermi level (E_F) - changes as in the case of doping with other atomic species. Hence, the characterization of the defect level is a prerequisite for understanding the electron transfer across the oxide-semiconductor interface, because the energy barrier height at the interface depends on E_F of the oxide^{1,2}. With regard to hafnium oxide, the energy position of this defect level has been estimated theoretically^{3,4,5} and experimentally^{6,7} to be above the middle of the bandgap, so E_F is shifted upward in the presence of oxygen vacancies. Since E_F is determined from the charge neutrality condition, it is largely influenced by the detailed density of states (DOS) near the bandgap¹; in this case, the intensity of the features near the conduction band (CB) is expected to be higher than those near the valence band (VB).

Recent density functional theoretical (DFT) studies^{3,4,5,8,9,10} have revealed that the defect state is the localized Hf d state. The nonzero occupation in Hf d shell is very natural, because Hf atom no longer donates electron to the adjacent vacant sites. If an inter-site correlation existed between the d -electrons, even a long-range correlation in the electronic configuration of each site might emerge. Surprisingly, room-temperature long range ferromagnetism (FM) was recently reported in an oxygen-deficient Hf oxide film^{11,12,13}, although an experimental counter-evidence shows the absence of FM¹⁴. Since the measured magnetization is the macroscopic quantity, it might significantly depend on the purity of the sample. Furthermore, recent DFT studies have revealed that FM can be induced by a hafnium vacancy rather than an oxygen vacancy, while the oxygen vacancy can at the most yield paramagnetism^{15,16,17}. Thus, it is important to investigate the possible long-range spin order in the oxygen-deficient $\text{HfO}_{x<2}$ from a *microscopic* point of view, in that the microscopic

quantities such as the spin or angular momentum drive the macroscopic properties, i.e., the magnetization. Since these microscopic values are determined from the electronic structure, the study on the local electron configurations of each atomic species will provide the information that is not influenced by a macroscopic deformation (domain interaction, dislocation, etc.) or an intervention of impurities.

Therefore, in this paper, we focus on electron redistribution and the possible long-range spin order in the presence of an oxygen vacancy in Hf-oxide by studying its electronic structure. To investigate the *unoccupied* electronic structure of Hf d states, we performed x-ray absorption spectroscopy (XAS) study on the $\text{HfO}_{x<2}$ film. Since XAS reflects a transition probability from a spatially localized core-level to the unoccupied levels, it is sensitive to the unoccupied states originating from the atoms near the photon-absorbing atom. Further, owing to the “locality” that allows transitions irrespective of momentum transfer, it reflects the momentum-averaged electronic structure that would be equivalent to the partial density of states (PDOS) in the absence of an electron correlation. We can choose the photon absorber by tuning the photon energy range to any of the core-level energies of each atomic species. Using the photon energy range $h\nu \sim 530$ eV, we can measure O K -edge ($1s \rightarrow 2p$) absorption to investigate the O $2p$ PDOS. Since parts of O $2p$ wavefunctions are hybridized with Hf $5d$ wavefunctions, O K -edge XAS also shows the unoccupied Hf $5d$ energy levels that are hybridized with the O wavefunctions. This implies that an Hf d -electron state that stays near the vacant site is hardly observed in O K -edge XAS. The situation is described in Fig. 1. The dashed circle near an oxygen atom roughly indicates the probing area of O K -edge XAS. However, at Hf N_3 -edge ($4p_{3/2}, h\nu \sim 380$ eV), we can detect all of the Hf $5d$ wavefunctions whether the d -electron state is localized near the vacancy or hybridized with the surrounding oxygen atoms (see Figure 1). Although the obtained spectra become complex due to the on-site core-hole effect, this measurement directly

shows the d -occupation at the Hf site.

The O K -edge and Hf N_3 -edge XASs of the oxygen deficient Hf oxide were performed at the 2A EPU6 beam line of the Pohang Light Source (PLS). In order to determine the existence of a long-range FM spin order, we also performed magnetic circular dichroism (MCD) measurements. The MCD spectrum is the difference between two XAS spectra measured using external magnetic field of mutually opposite directions. Here, a circularly polarized photon should be used, since the relative orientation of its chirality with respect to the direction of the spin moment determines the preference of pumped spin. To align the spin direction, the magnetic field exceeding the coercivity field of the system should be applied. The oxygen-deficient film of ~ 20 Å was fabricated onto HF-etched Si(100) substrate with a 3 Hz pulsed Nd:YAG laser at a substrate temperature of 700 °C. The base pressure of the growth chamber was 1×10^{-8} Torr and no oxygen flow was supplied during the film growth. The oxygen concentration deduced from the intensity ratio of O $1s$ /Hf $4f$ core-levels in the *in situ* x-ray photoemission spectroscopy (XPS) spectra was approximately 1.8 (i.e., 10% oxygen deficiency). An approximate estimation of the Hf valence leads to $\sim \text{Hf}^{3.6+}$, i.e., a composite of 60% of Hf^{4+} and 40% Hf^{3+} .

Figure 2 shows the O K -edge XAS spectrum with circularly polarized photons for $\text{HfO}_{1.8}$. The overall features of the spectrum are similar to those of the previous experiments for HfO_2 ^{18,19,20} as well as the theoretical band calculations for the unoccupied states^{10,21,22,23}. The spectrum was analyzed using a model cluster calculation with full atomic multiplets²⁴, assuming the composite [d^0 (60%) \oplus d^1 (40%)] in a perfect monoclinic crystal structure. As already noted, XAS is relevant to the interactions between the near atoms only; therefore, the single cluster model with an Hf atom and its nearest oxygen atoms is sufficient to simulate the XAS spectra. Though the Hf oxide film is in an amorphous phase, the local bonds can be assumed to be similar to those of the bulk monoclinic structure²⁵. The crystal field (CF) split energy ratios were calculated based on the bulk crystal structure, and the overall CF splitting energy was used as a variable scaling parameter to fit the experimental XAS spectra. The one-electron energy level for $\text{Hf } 5d^0 \rightarrow 5d^1$ (empty bars in Fig. 2) is analyzed to be composed of five non-degenerate states: $^2D(xy/x^2 - y^2)$, $^2S(3z^2 - r^2)$, $^2P(xz/yz)$, and two mixed states in the increasing order of energy. (Here the coordinate is taken as in Fig. 2.) The intensities of the five d levels are multiplied by the Hf $5d$ -O $2p$ hybridization strength using the Harrison's rule (exponent -7 for different interatomic distances)²⁶ for the local structure as shown in the figure. The hybridization strength was found to exhibit an anisotropy; the in-planar 2D state has much weaker hybridization strength than the other levels ($\sim 20\%$ of 2S and 2P 's). The $5d^1 \rightarrow 5d^2$ simulation (filled bars) shows the similar results, except an overall broadening of features due to the atomic multiplets in the d^2 final state²⁷. The spectra

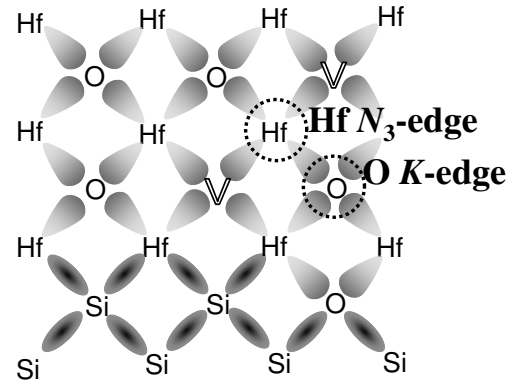


FIG. 1: Schematic diagram of the atomic distribution of $\text{HfO}_{x<2}/\text{Si}$. For simplicity, all the bonds are assumed to be four-fold. Lobes indicate the inter-site wavefunction overlaps. The shape and darkness in each lobe represent the electron density. The dashed circles indicate the spatial extent to which each XAS spectrum could detect the electronic structure. In O K -edge XAS, it is impossible to observe the localized Hf d -electron state near the oxygen vacancy (denoted as “V”), if it were not for the delocalization of the wavefunctions, in contrast to the Hf N_3 -edge XAS.

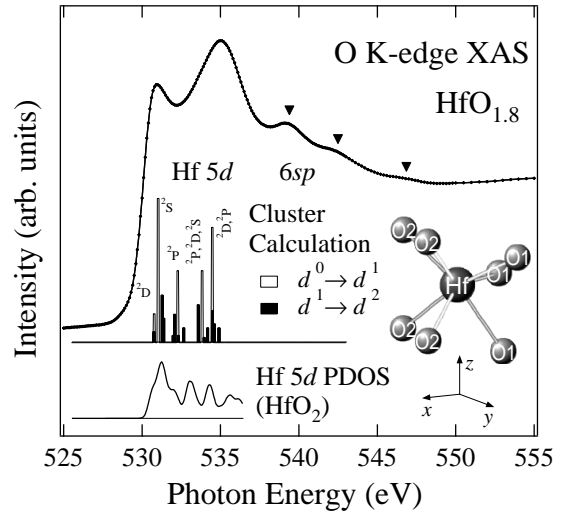


FIG. 2: Unoccupied DOS of $\text{HfO}_{1.8}$ probed by O K -edge XAS with circularly polarized photons. The results of the atomic single cluster model calculations [$d^0(d^1) \rightarrow d^1(d^2)$] are also shown as empty (filled) bars. The cluster considered in this study is shown in the inset. For comparison, the Hf $5d$ PDOS of HfO_2 taken from Ref.¹ is shown at the bottom of figure.

simulated with the overall CF energy of approximately 4 eV, agree with the experimental spectrum and with the calculated Hf $5d$ PDOS¹ shown in Fig. 1.

A slight difference in the XAS spectra of the oxygen-deficient film from the stoichiometric film can be seen in the features near the bandgap as shown in Fig. 3. For comparison, we appended the XAS spectrum of the

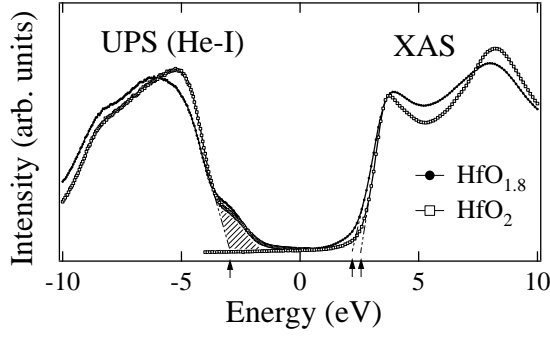


FIG. 3: Combined (normalized) UPS and XAS spectra of $\text{HfO}_{1.8}$ and stoichiometric HfO_2 , for DOS near the bandgap. The UPS spectrum for $\text{HfO}_{1.8}$ is taken from Ref.³². Here, the position of the chemical potentials (zero energy in the figure) for both UPS and XAS spectra were arbitrarily chosen to be approximately in the middle of the bandgap, preserving the bandgap of *bulk* HfO_2 (~ 5.7 eV). Dotted lines show the extrapolations to obtain the approximate energy positions (arrows) of the CB and VB edges, and the shaded area indicates the contributions of the Si substrate or the interface state.

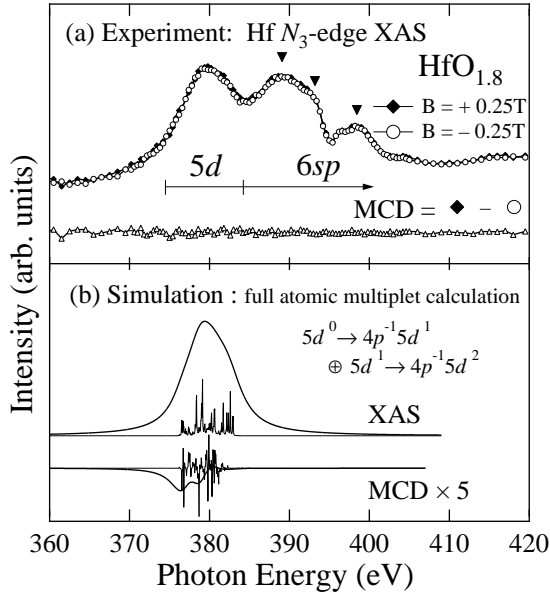


FIG. 4: (a) Hf $N_{3\text{-edge}}$ XAS with circularly polarized photons. The difference spectrum or MCD has no feature, indicating no long-range FM spin-order. The results of the atomic cluster model calculations for the composite of d^0 (60%) \oplus d^1 (40%) are also shown in (b).

stoichiometric HfO_2 film measured under the same conditions. Both spectra were normalized approximately preserving the total absorption intensity. The spectrum of oxygen-deficient film appears broader than that of the stoichiometric one. We checked the broadness for many measurement points on each sample and found the consistency for each sample. Thus, the broadness can be

regarded as an intrinsic property of the oxygen-deficient film. Though no prominent gap state is observed in the XAS spectrum of the oxygen-deficient film, the CB edge extends toward the bandgap as compared to the stoichiometric one. This can be interpreted as the partial delocalization of the defect state; that is, the defect state might be rather dispersed so that it can also be detected at the oxygen site. Thus, the role of the oxygen vacancy can be regarded as donating electron back to the Hf site and consequently to the O site through the Hf–O hybridization. In particular, when the vacancy is at the HfO_2/Si interface, it is easily substituted by the Si atom to form an O–Hf–Si bonding. This could also slightly enhance the Hf d occupation, although its amount is reduced due to the electron transfer to the Si site²⁸. However, the CB tail cannot be attributed to the formation of a direct O–Si bonding. This is because the bandgap of SiO_2 (~ 9 eV) is much larger than of HfO_2 (~ 5.7 eV); therefore, no structure can exist near the bandgap. We can expect that the bandgaps of any types of the their intermediate state, i.e. the silicate ($\text{Hf}_x\text{Si}_y\text{O}_4$) will be between these two values^{29,30}, resulting in the absence of states inside the HfO_2 bandgap. Therefore, it is evident that the lack of oxygen atom in the oxide or at the interface is responsible for the occurrence of the CB tail state²³.

If degree of amorphousness in the Hf-oxide is somehow enhanced, this could also extend the CB edge due to the broadening of the features³¹. In this case, the tailing should occur in both the VB and CB edges. In the following paragraph, however, we will show that the tailing does not occur in the VB edge; this manifest that the CB tail is truly caused by the physics of defects, not by the uncertainty in the lattice dynamics³¹.

To verify the existence of the band-tails in the *occupied* DOS, we also performed ultraviolet photoemission spectroscopy (UPS) using He–I ($h\nu = 21.2$ eV) light source for both the films. (The UPS spectrum for $\text{HfO}_{1.8}$ is taken from Ref.³².) The UPS spectra are also normalized with respect to the total intensity. Here, the energy zero is arbitrarily chosen to approximately sustain the energy difference between the lowest XAS edge ($\sim +2.5$ eV) and the highest UPS main feature ($\lesssim -3$ eV) to be the known bandgap of HfO_2 (~ 5.7 eV; Ref.³³). The UPS spectrum of $\text{HfO}_{1.8}$ film is shifted by $+0.3$ eV in order to compensate for the E_F shift in the oxide, which was obtained from the cutoff kinetic energies of the secondary electrons in the spectra (not shown here)³²; this E_F shift induces the higher binding energy (BE) shift in the photoemission spectra, because the BE is, by definition, the energy difference between the Fermi level and the core level, while XAS is independent of the E_F position because the energy difference between the initial core level and the final conduction level is independent of the Fermi level. The large and broad features around the relative energy of $-8 \sim -4$ eV correspond to the main O $2p$ occupied state, while the tail toward the bandgap (shaded area at around -3 eV in Fig. 3) probably originates from

the underlying Si wafer³⁴, because this VB tail is absent in the UPS spectra of thicker (> 100 Å) HfO_2 film (not shown here). A slight increase in the tail in the oxygen deficient film might be a signature of the metallic Hf silicide (Hf–Si bond) at the interface³⁵. However, the VB edge of the oxygen-deficient film does not extend inside the bandgap as compared with that of the stoichiometric sample. Though it is difficult to unambiguously analyze these band-tail states in both the occupied and unoccupied DOSs, we can observe that only the unoccupied DOS near the bandgap tends to extend inside the bandgap in the presence of oxygen vacancy^{10,21}. This result should be correlated with the lifting of Fermi level because the virtual transition to CB becomes easier.

Up to this point, we have shown experimental evidence that the oxygen vacancy lowers the CB edge and increases the effective Fermi level. The detailed mechanism explaining how the vacancy formation lowers the CB edge could be revealed by a further consideration of the atomic rearrangements or the relaxation following the vacancy formation. For example, the disorder in the positions of the vacant sites can play a role in broadening the CB DOS and consequently in reducing the bandgap. Further, the energy position of the defect level is found to depend on the atomic arrangements after the vacancy formation³. The reduction in the mean Hf–O bond length (~ 0.1 Å) and in the number of bonds, in the presence of oxygen vacancy³², will influence the detailed balance in the charge dynamics between the two atomic species. The CB lowering can also be correlated with the broadening of features influenced by the valence configurations (the number of electrons) of the remaining atoms, as shown in the simulation results in Fig. 2. Further investigation is required to completely understand the mechanism.

Now we check if there be a long-range FM spin order. The Hf N_3 -edge XAS spectra obtained with circularly polarized photons are shown in Fig. 4(a). The external magnetic field was maintained perpendicular to the sample plane with $H = \pm 2500$ Oe, which is much larger than the reported ferromagnetic coercivity field of the HfO_2 film¹¹. The difference spectrum, i.e., the MCD spectrum exhibits no clear feature and remains zero within the experimental uncertainty. This indicates that there is no Hf d -electron-related FM spin order. One would argue that the density of the oxygen vacancy is too small to detect FM; however, the value of 10% is larger than the dopant density in conventional diluted magnetic semiconductors (DMS)³⁶.

To analyze the spectral features, we appended in Fig.

4(b) the simulation result obtained by the full atomic multiplet calculation for Hf N_3 -edge XAS ($4p_{3/2} \rightarrow 5d$) with the parameters similar to that of O K -edge XAS, except the $4p-5d$ Coulomb interactions³⁷. As was in the O K -edge XAS simulation, the simulated spectra are obtained by the sum of two transitions: $5d^0 \rightarrow 4p^5 5d^1$ and $5d^1 \rightarrow 4p^5 5d^2$. The features of the latter are shifted by $U - F_{pd}^0 = -2$ eV³⁷ with respect to those of the former. The result of the calculation is in an excellent agreement with the experimental spectra; therefore, it provides definite peak assignments; the Hf $4p_{3/2} \rightarrow 5d$ transition is the largest feature, while the other features in the higher photon energies are attributed to the Hf $4p_{3/2} \rightarrow 6sp$ transition. Contrary to $2p \rightarrow 3d$ transition (as in the case of transition metal ions), the feature of Hf $4p \rightarrow 5d$ transition is not much stronger than $4p \rightarrow 6sp$, because of its lower photo-absorption cross-sections. The features of Hf $6sp$ for both the edges are denoted by \blacktriangledown in Figs. 2 and 4. The peak positions almost coincide, confirming our peak assignments. The simulated MCD signal for Hf $5d$ [Fig. 4(b)] is small due to the small anisotropy in the unoccupied electron states (d^{8-9}). Although the sensitivity of the MCD measurement on magnetism is low, no correlation was observed between the experimental and simulated MCD spectra. This confirms that the small modulation in the experimental spectrum is caused by the noise, not the possible long-range magnetism.

Therefore, we can conclude that there is no preference in spin selection in the electron occupation to either Hf $5d$ or $6sp$; this evidently proves “no ferromagnetic spin-order” in the case of oxygen vacancy. However, the electron occupation number at an Hf site should be nonzero; otherwise, the electronic configurations of the next nearest O sites, which was shown in O K -edge XAS spectra (Fig. 3), should never be influenced by the presence of oxygen vacancy. Thus, the absence of FM spin-order can be explained by the absence of long-range correlation between the d -electrons in the neighboring Hf sites, rather than the absence of d -electron itself.

We conclude our arguments with two remarks: the oxygen vacancy in Hf oxide slightly enhances the CB DOS. However, it does not involve the long-range ferromagnetic spin order in the oxide because of the absence of inter-site electron correlation.

This study is supported by the Korean Science and Engineering Foundation through the Center for Strongly Correlated Materials Research at the Seoul National University, and the experiments at PLS were supported in part by MOST and POSTECH.

* Electronic address: sjoh@plaza.snu.ac.kr

¹ P. W. Peacock and J. Robertson, J. Appl. Phys. **92**, 4712 (2002).

² Y.-C. Yeo, T.-J. King, and C. Hu, J. Appl. Phys. **92**, 7266 (2002).

³ K. Xiong, J. Robertson, M. C. Gibson, and S. J. Clark,

Appl. Phys. Lett. **87**, 183505 (2005).

⁴ J. L. Gavartin, D. M. Ramo, A. L. Shluger, G. Bersuker, and B. H. Lee, Appl. Phys. Lett. **89**, 082908 (2006).

⁵ J. Robertson, K. Xiong, and S. J. Clark, Thin Solid Films **496**, 1 (2006).

⁶ H. Takeuchi, D. Ha, and T.-J. King, J. Vac. Sci. Technol.

- A **22**, 1337 (2004).
- ⁷ A. Kerber, E. Cartier, L. Pantisano, R. Degraeve, T. Kauerauf, Y. Kim, G. Groeseneken, H. E. Maes, and U. Schwalke, *IEEE Electron Device Lett.* **24**, 87 (2003).
 - ⁸ J. X. Zheng, G. Ceder, T. Maxisch, W. K. Chim, and W. K. Choi, *Phys. Rev. B* **75**, 104112 (2007).
 - ⁹ J. Kang, E.-C. Lee, and K. J. Chang, *Appl. Phys. Lett.* **84**, 3894 (2004).
 - ¹⁰ E. Cockayne, *Phys. Rev. B* **75**, 94103 (2007).
 - ¹¹ M. Venkatesan, C. B. Fitzgerald, and J. M. D. Coey, *Nature* **430**, 630 (2004).
 - ¹² J. M. D. Coey, M. Venkatesan, P. Stamenov, C. B. Fitzgerald, and L. S. Dorneles, *Phys. Rev. B* **72**, 024450 (2005).
 - ¹³ N. H. Hong, J. Sakai, N. Poirot, and V. Brizé, *Phys. Rev. B* **73**, 132404 (2006).
 - ¹⁴ D. W. Abraham, M. M. Frank, and S. Guha, *Appl. Phys. Lett.* **87**, 252502 (2005).
 - ¹⁵ C. Das Pemmaraju and S. Sanvito, *Phys. Rev. Lett.* **94**, 217205 (2005).
 - ¹⁶ G. Bouzerar and T. Ziman, *Phys. Rev. Lett.* **96**, 207602 (2006).
 - ¹⁷ H. Weng and J. Dong, *Phys. Rev. B* **73**, 132410 (2006).
 - ¹⁸ S. Toyoda, J. Okabayashi, H. Kumigashira, M. Oshima, K. Yamashita, M. Niwa, K. Usuda, and G. L. Liu, *J. Appl. Phys.* **97**, 104507 (2005).
 - ¹⁹ G. Lucovsky, Y. Zhang, G. B. Rayner, Jr., G. Appel, H. Ade, and J. L. Whitten, *J. Vac. Sci. Technol. B* **20**, 1739 (2002).
 - ²⁰ M.-H. Cho, D. W. Moon, S. A. Park, Y. K. Kim, K. Jeong, S. K. Kang, D.-H. Ko, S. J. Doh, J. H. Lee, and N. I. Lee, *Appl. Phys. Lett.* **84**, 5243 (2004).
 - ²¹ A. S. Foster, F. Lopez Gejo, A. L. Shluger, and R. M. Nieminen, *Phys. Rev. B* **65**, 174117 (2002).
 - ²² A. B. Mukhopadhyay, J. F. Sanz, and C. B. Musgrave, *Phys. Rev. B* **73**, 115330 (2006).
 - ²³ K. Xiong, P. W. Peacock, and J. Robertson, *Appl. Phys. Lett.* **86**, 12904 (2005).
 - ²⁴ A. Tanaka and T. Jo, *J. Phys. Soc. Jpn.* **61**, 2040 (1992).
 - ²⁵ R. Ruh and W. R. Corfield, *J. Amer. Ceram. Soc.* **53**, 126 (1970).
 - ²⁶ W. A. Harrison, *Electronic Structure and the Properties of Solids* (Freeman, San Francisco, 1980).
 - ²⁷ Here the effect of charges generated by the oxygen vacancy is neglected, so that the overall CF splitting energy is assumed to be independent of the number of d -electrons.
 - ²⁸ M. S. Joo, B. J. Cho, N. Balasubramanian, and D. L. Kwong, *IEEE Electron Device Lett.* **25**, 716 (2004).
 - ²⁹ H. Kato, T. Nango, T. Miyagawa, T. Katagiri, K. S. Seol, and Y. Ohki, *J. Appl. Phys.* **92**, 1106 (2002).
 - ³⁰ Y. Kamimuta, M. Koike, T. Ino, M. Suzuki, M. Koyama, Y. Tsunashima, and A. Nishiyama, *Jpn. J. Appl. Phys.* **44**, 1301 (2005).
 - ³¹ P. W. Anderson, *Phys. Rev.* **109**, 1492 (1957).
 - ³² D.-Y. Cho, C.-H. Min, J. Kim, S.-J. Oh, and M.-G. Kim, *Appl. Phys. Lett.* **89**, 253510 (2006).
 - ³³ M. Balog, M. Schieber, M. Michman, and S. Patai, *Thin Solid Films* **41**, 247 (1977).
 - ³⁴ S. Sayan, T. Emge, E. Garfunkel, X. Zhao, L. Wielunski, R. A. Bartynski, D. Vanderbilt, J. S. Suehle, S. Suzer, and M. Banaszak-Holl, *J. Appl. Phys.* **96**, 7485 (2004).
 - ³⁵ D.-Y. Cho, K.-S. Park, B.-H. Choi, S.-J. Oh, Y. J. Chang, D. H. Kim, T. W. Noh, R. Jung, and J. C. Lee, *Appl. Phys. Lett.* **86**, 041913 (2005).
 - ³⁶ J. M. D. Coey, M. Venkatesan, and C. B. Fitzgerald, *Nat. Mater.* **4**, 173 (2005).
 - ³⁷ Here the Slater integrals for $\text{Hf}^{3+}(d^1)/\text{Hf}^{2+}(d^2)$ final states were taken as the reduced values by less than half from those calculated for $\text{Hf}^{3+}/\text{Hf}^{2+}$ ion by using Cowan's code for Hartree-Fock method: for $\text{Hf}^{3+}(d^1)$, $F_{pd}^2=9.447$, $G_{pd}^1=2.187$, and $G_{pd}^3=2.239$ in eV; and for $\text{Hf}^{2+}(d^2)$, $F_{dd}^2=13.102$, $F_{pd}^4=9.086$, $F_{pd}^2=9.332$, $G_{pd}^1=2.124$, and $G_{pd}^3=2.183$ in eV. Hubbard U and F_{pd}^0 were set to 2 eV and 4 eV, respectively, and the $5d$ spin-orbit coupling constant was set to about 0.1eV throughout the calculation. For more details of the calculational method, refer to R. D. Cowan, *The Theory of Atomic Structure and Spectra* (Univ. of California Press, 1981).